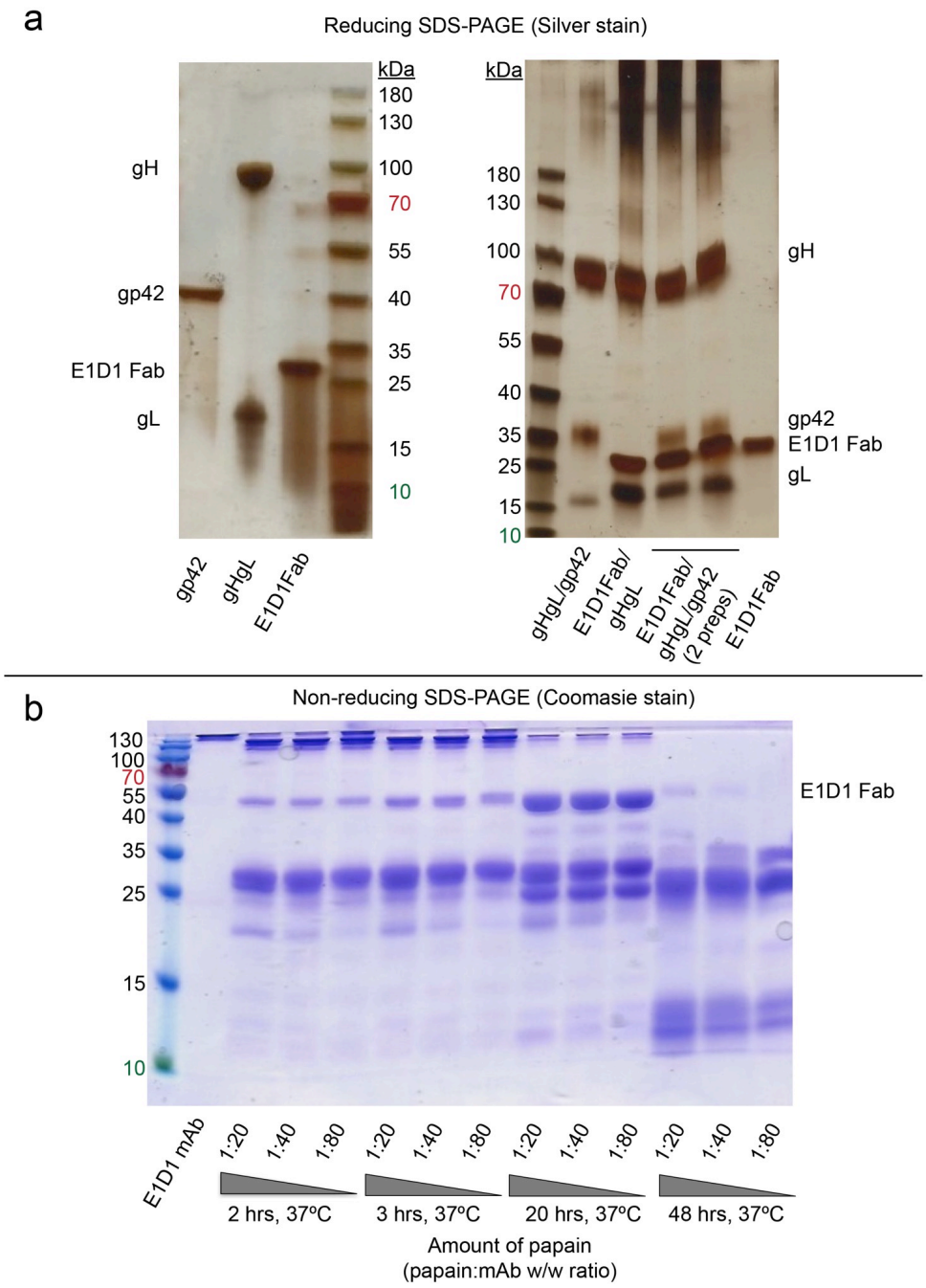

Supplementary Figure S1. Characterization of gHgL/gp42/E1D1 complex and generation of 50 kDa Fab fragment by controlled enzymatic digestion of E1D1. (**a**) SDS-PAGE analysis under reducing conditions (silver-stain) of gHgL, gp42, and E1D1 Fab complexes. (**b**) SDS-PAGE analysis under non-reducing conditions (coomasie stain) for generation of E1D1 Fab from intact E1D1.

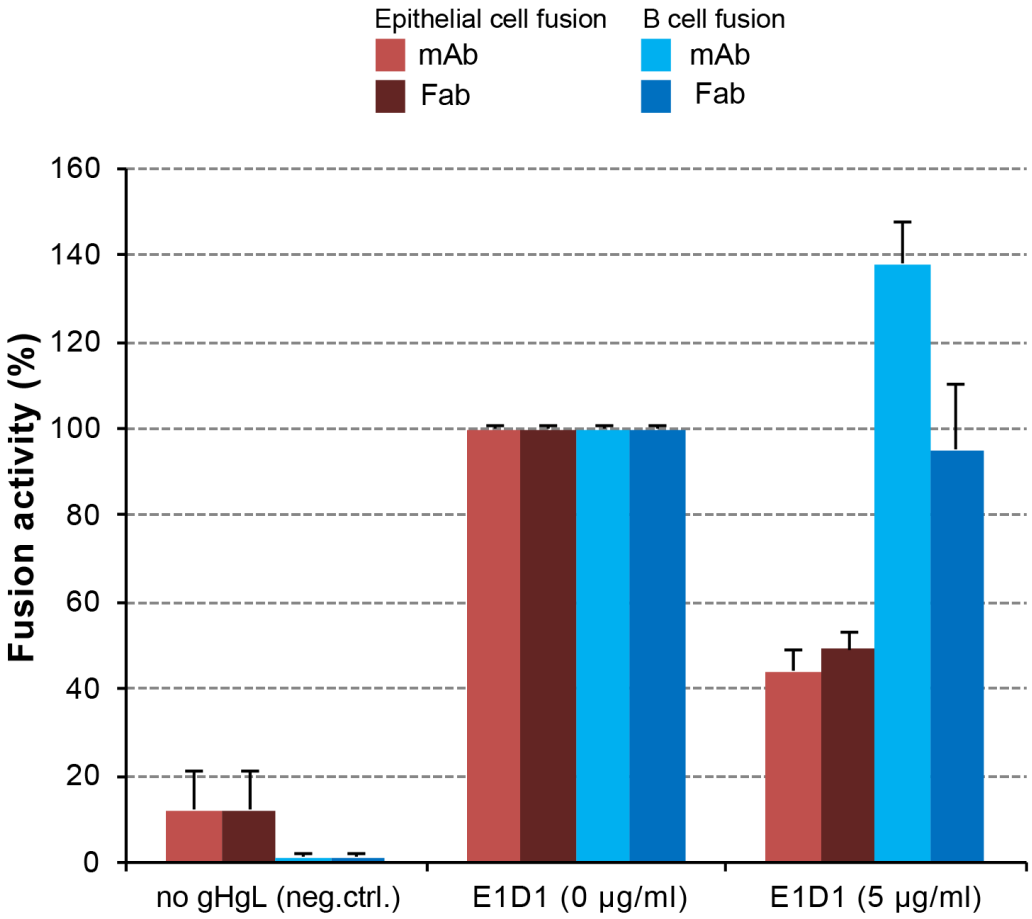

Supplementary Figure S2. Partial inhibition of epithelial cell fusion activity by E1D1 Fab and mAb. Epithelial cell fusion activity is represented as the average of three biological replicates and shown as maroon histogram bars. B cell fusion activity is similarly shown as blue bars. Lighter shades denote addition of mAb and darker shade denote Fab addition during the fusion assay. Error bars are ±S.D. (Standard Deviation).

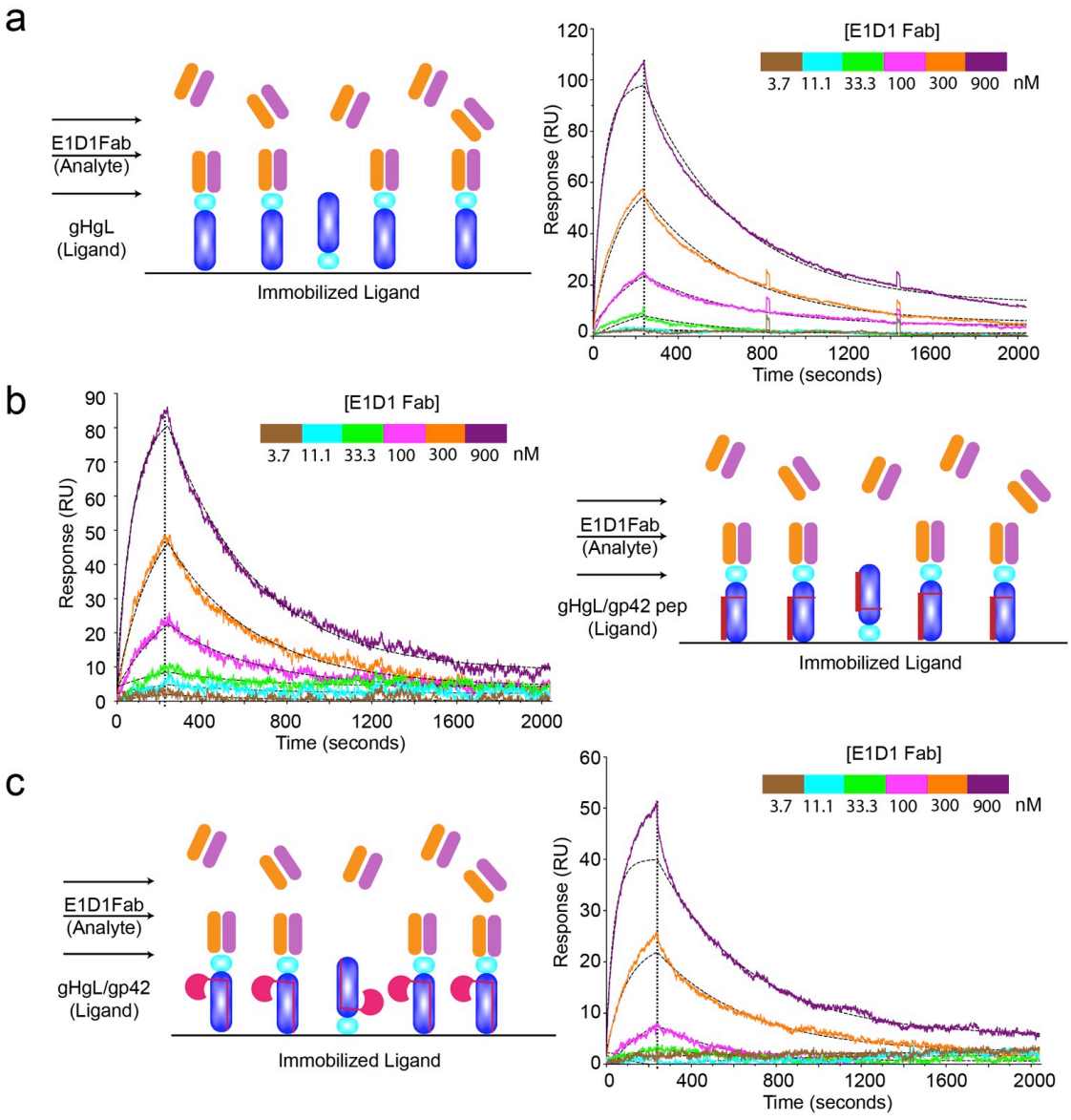

Supplementary Figure S3. E1D1 affinity for gHgL is not affected by gp42 or gp42-peptide. Surface Plasmon Resonance (SPR) measurements of E1D1 Fab binding to (**a**) gHgL, (**b**) gHgL/N-domain peptide and (**c**) gHgL/gp42. gHgL, gHgL/gp42pep, or gHgL/gp42 was used as the immobilized ligand while E1D1 Fab was used as the soluble analyte (mobile phase). The kinetics data (on-rate and off-rate) and affinity (K_D) values from a global fit of a 1:1 interaction model are collected in Table 1.

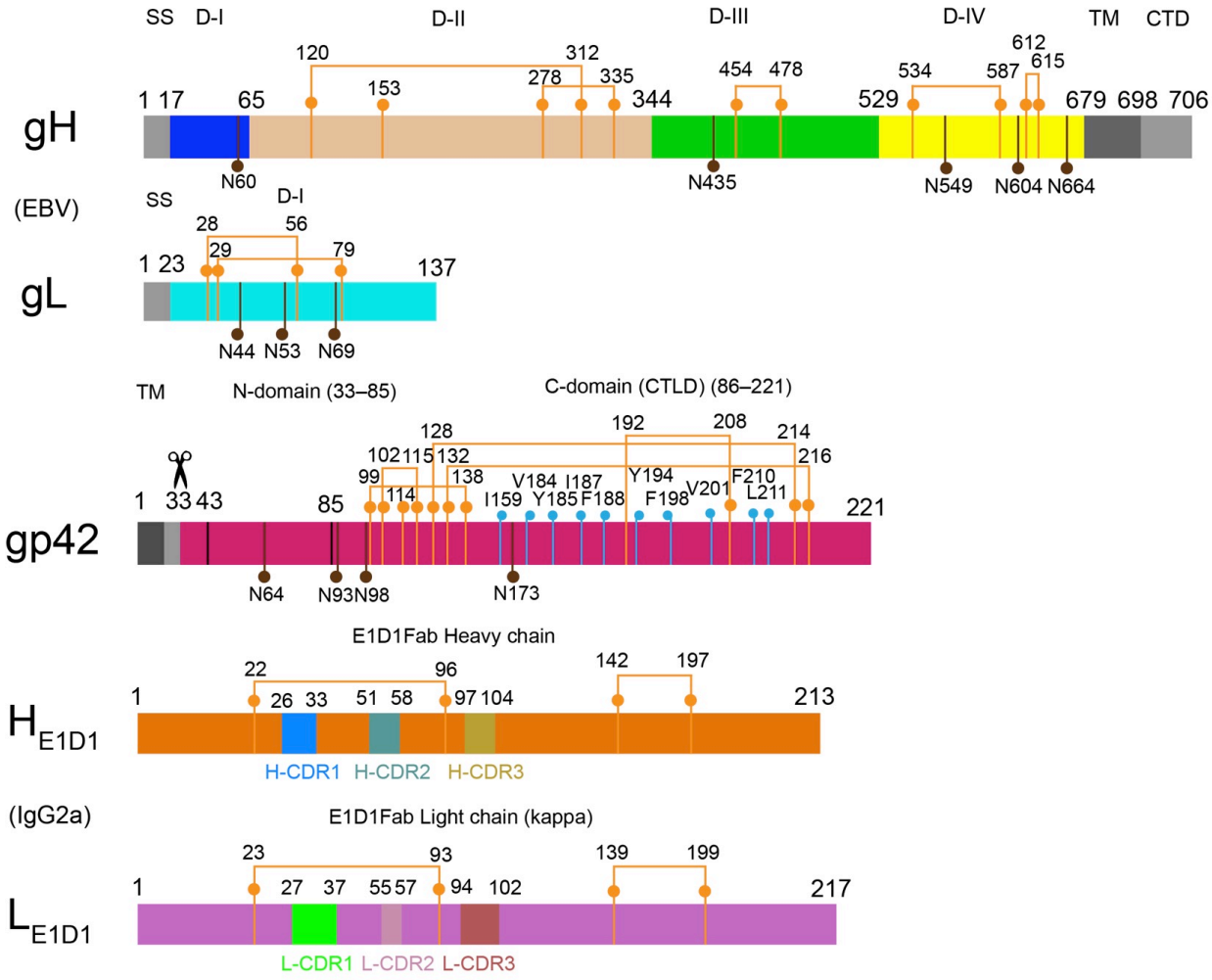

Supplementary Figure S4. Schematic representations of gHgL, gp42 and E1D1 Fab proteins. The 2-D bars represent the domain boundaries of gH, gL, gp42 and E1D1 Fab. The bar diagrams of individual domains are colored using the same coloring scheme as in Fig. 2. Potential N-linked glycosylation sites are labeled and numbered by downward pointing brown 'lollipops' and cysteines are numbered and shown as upward pointing orange 'lollipops'. Orange connected horizontal lines show disulfide bridges. C153 in gH D-II and C114 in gp42 are unpaired cysteines. The cleavage site for the gp42 N-terminal anchor is shown by a scissor. SS stands for signal sequence, TM for transmembrane and CTD for C-terminal domain.

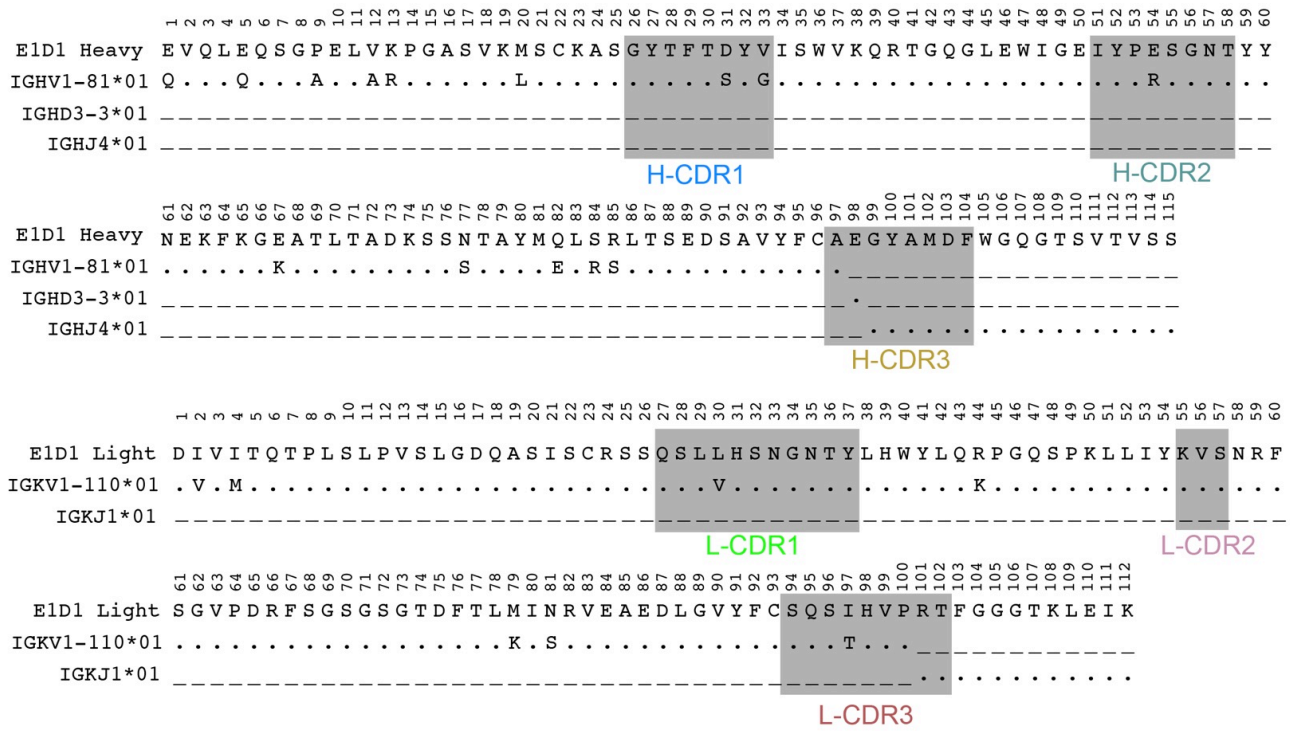

Supplementary Figure S5. Sequences of the E1D1 V_H and V_L domains. The amino acid sequence of E1D1 heavy and light chain was obtained using cDNA isolated from E1D1 expressing hybridoma cells. The alignment shows the closest V-D-J allelic regions for the heavy and V-J regions for the light chain (imgt.org/IMGT_vquest) giving the inferred unmutated common ancestor (UCA) sequence. Dot '.' denotes identity and dash '-' denotes a gap. Residues that differ due to presumed somatic mutation are represented by the original amino acid single letter code in the alignment. Grey box background highlights the E1D1 Complementarity Determining Regions (CDRs). The heavy chain CDRs are labeled H-CDR1 through 3 and the light chain CDRs are labeled L-CDR1 through 3. Coloring scheme for the CDR labels is identical to the coloring for those regions in the structure as represented in Fig. 5 and in Supplementary Fig. S4.

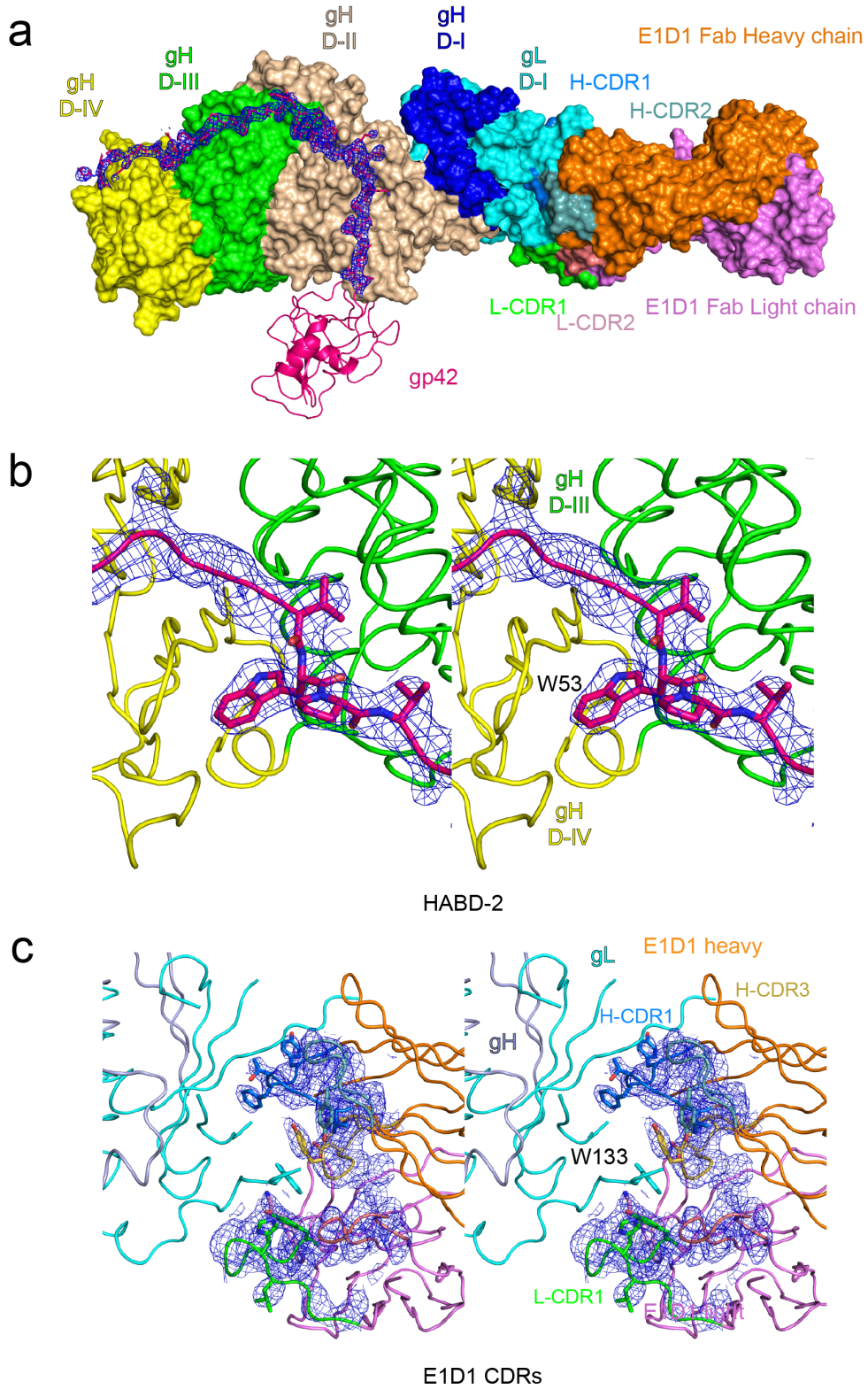

Supplementary Figure S6. Examples of electron density observed for gp42 and E1D1 model building. Simulated annealing (SA) composite omit maps contoured at 1.0 σ for (**a**) gp42 N-domain (43–85), (**b**) High Affinity Binding Determinant 2 (HABD-2) as from Fig. 3c, and (**c**) E1D1 CDR's showing the correspondence with the modeled amino acids in those spatial positions as in the crystal structure. Panels (**b**) and (**c**) are shown as stereo pairs.

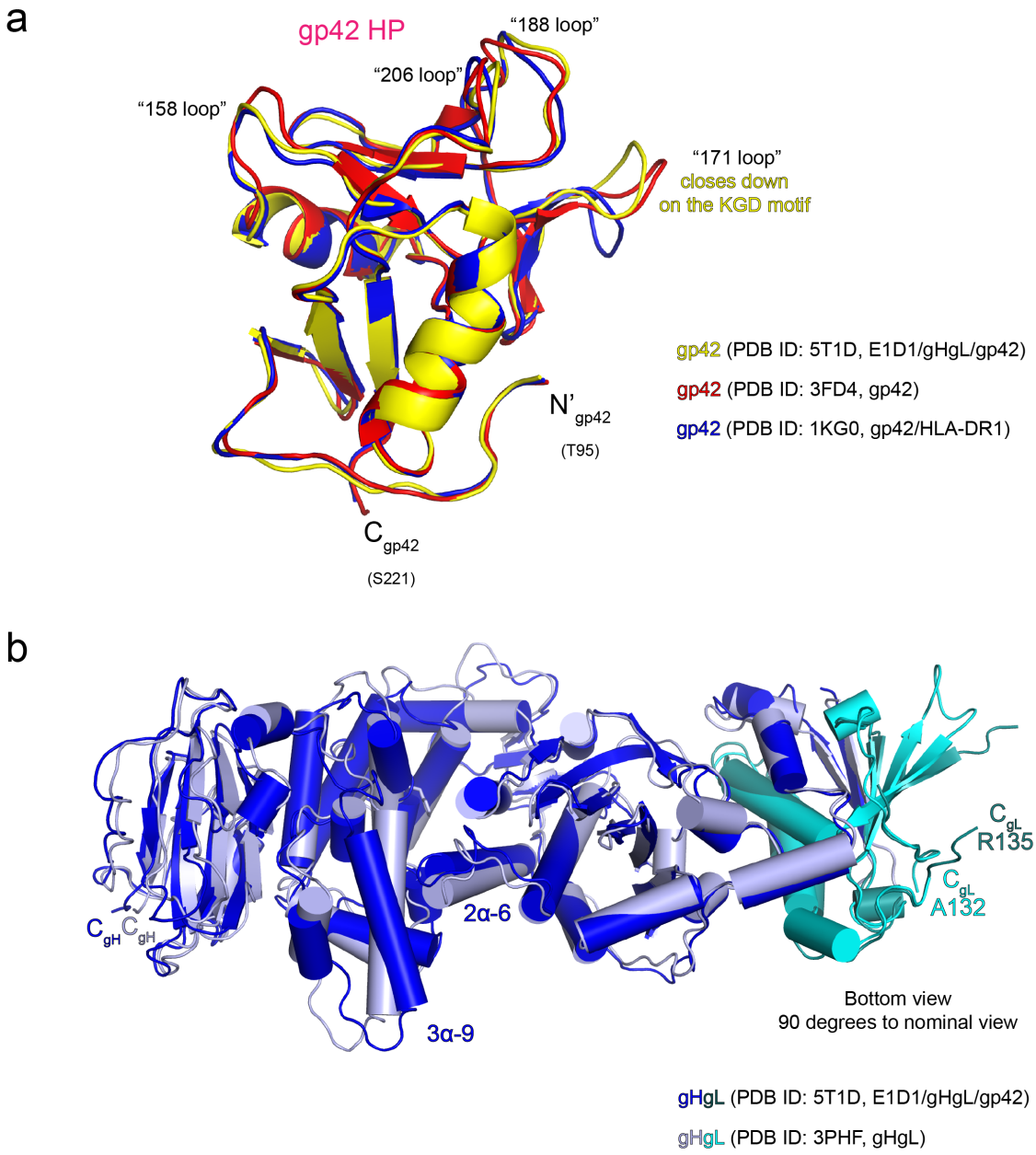

Supplementary Figure S7. Structural differences in EBV gHgL and gp42 in known crystal structures. Structural alignments for (**a**) gp42, and (**b**) gHgL from different crystal structures highlighting notable differences. Legends to denote the coloring of different domains is included in each panel within the figure.

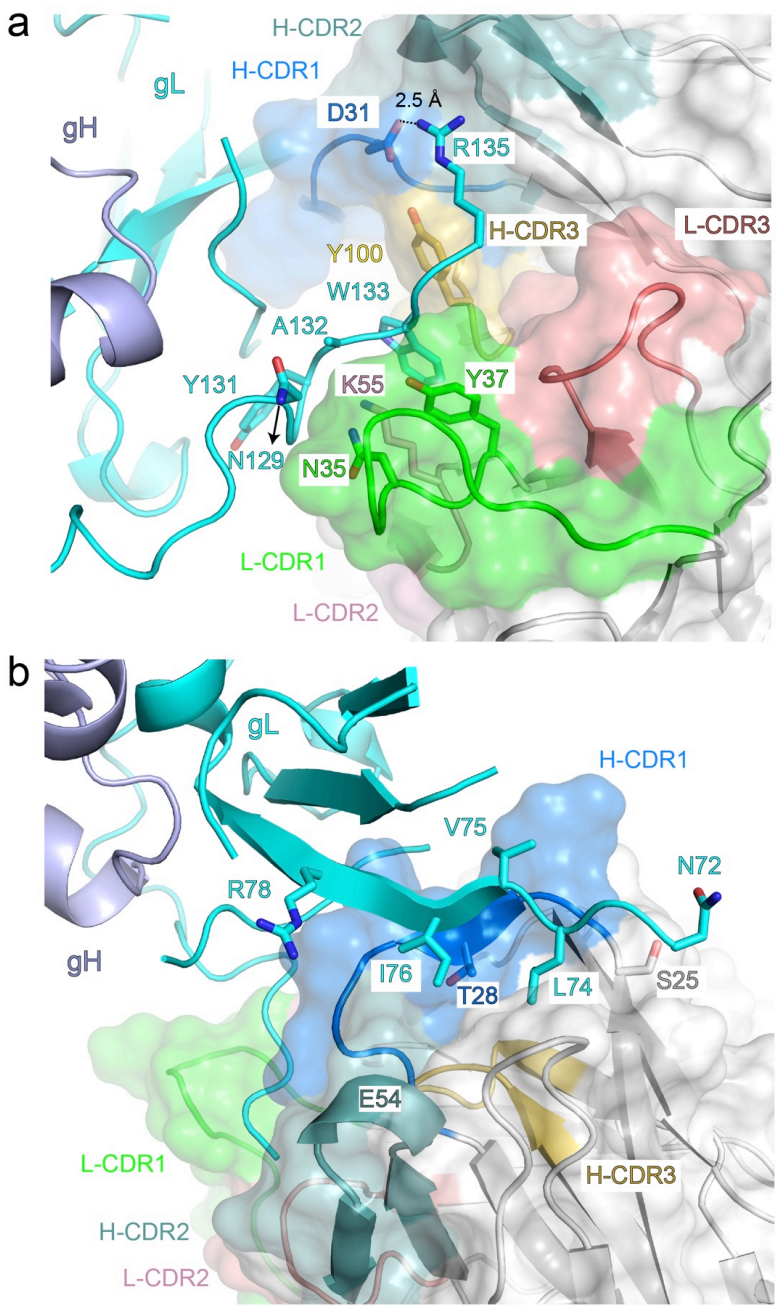

Supplementary Figure S8. Interactions of E1D1 residues with gL. (**a**) Interactions between gL and E1D1 residues shown in stick format. (**b**) Interactions between gL β-3 strand (Lβ-3, residues 72–79) and E1D1 heavy chain CDR. gL:L74–I76 is buried in a shallow hydrophobic cleft within H-CDR1. For all panels H-CDR1 is colored marine, H-CDR2 is lightteal, H-CDR3 is sulfur; and, L-CDR1 is green, L-CDR2 is pink, and L-CDR3 is deepsalmon (coloring scheme label as from Pymol). gH is colored lightblue and gL in cyan. Structures were rendered using MacPyMol.

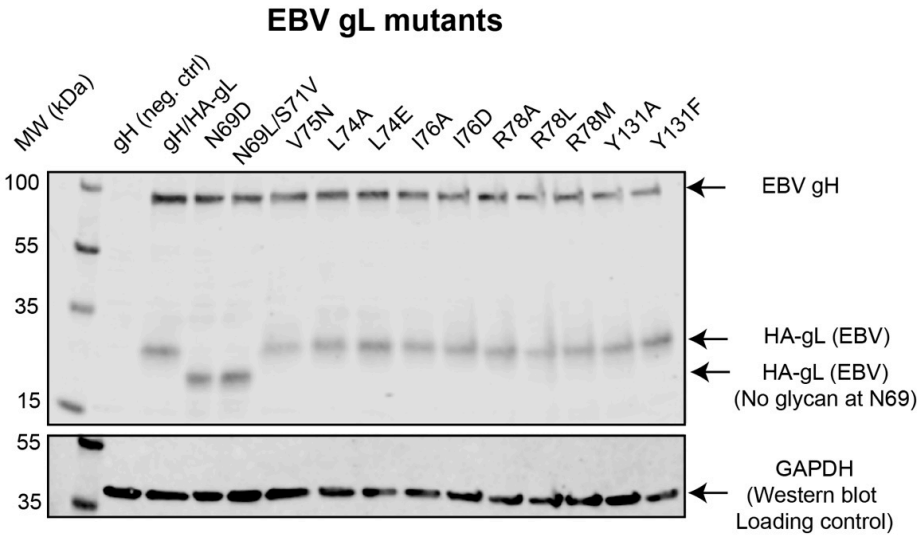

Supplementary Figure S9. Expression levels of different gL mutants. Western blot of gHgL mutants detected using a polyclonal anti-gHgL antibody (rabbit). GAPDH bands are shown as a loading control and shows similar levels of expression of all mutants tested in the cell-cell fusion assays (Fig. 6).

Supplementary Table S1. EBV gH residue contacts with gp42 N-domain. Gp42 residues (43–85) are arranged in descending order of the most buried, non-zero difference in Accessible Surface Area (ASA) as calculated by naccess, 76 gH residues contact gp42 N-domain.

Structural feature (gH subsite)	gH residue	Buried surface area (Change in ASA) (Å^2)	Nearby gp42 residues
HABD-4	Y132	107.91	E68, Y71, G72, D73
Linker	R350	102.18	F63, N64, K65
HABD-2	E362	87.16	V52
HABD-4	Y346	79.23	A67, E70, Y71
HABD-4	Y133	76.29	Y71, D73, V76
Turn between HABD-1–3 and HABD-4–5	I134	75.27	K74, E75
HABD-1	I613	72.60	W44, P46
HABD-3	Y389	63.98	P57, P58, P59
HABD-2	I548	62.35	W53
HABD-5	Y157	51.56	V76, L78, P79
HABD-5	T170	50.59	L78, P79, W81
HABD-1	C615	48.68	K47, P48, N49
HABD-5	Q168	47.85	W81
HABD-2	N442	45.91	V52, W53, P54
HABD-5	D165	44.75	W81, T82, T84
HABD-4	Q344	42.80	Y71
HABD-2	L401	39.58	N49, V50, E51
HABD-2	P441	38.63	W53
HABD-2	T635	36.37	N49, V50, E51
HABD-5	V185	35.09	P83
HABD-1	F617	34.01	K47
HABD-1	C612	32.45	P46, K47
Linker	P109	31.37	F63
HABD-2	L445	31.17	W53
HABD-5	T136	26.37	K77

HABD-3	Y383	25.65	P59, P60
Linker	M354	25.41	F63
HABD-3	V388	24.31	P59, P60
D-I/D-II groove	R152	22.90	E75
HABD-5	E187	22.54	L85, H86
HABD-3	A357	22.52	P58, P59
HABD-5	S161	20.63	W81
HABD-2	S636	19.74	N49
HABD-3	A353	19.60	P60, V61
HABD-1	S611	17.95	P46
HABD-5	A159	17.94	P79
HABD-3	Q439	17.92	V55
HABD-5	G135	17.57	V76, K77
HABD-5	K341	17.50	V76
HABD-1	I602	16.96	W44
HABD-5	K166	16.23	T84, L85, H86
HABD-1	F614	15.69	W44
HABD-5	G164	14.25	T84
HABD-3	G391	14.09	V55
HABD-5	L155	13.77	K77, L78
Linker	V107	12.52	F63
HABD-1	T663	11.32	K47, P48
HABD-5	A172	10.87	L78
HABD-1	M668	10.39	W44
HABD-1	Q609	9.45	W44
HABD-1	F605	8.85	W44
HABD-1	G616	8.52	K47
HABD-5	L160	8.14	W81

HABD-4	Q129	8.04	Y71
HABD-2	Q637	7.67	N49
HABD-3	M361	7.01	D56, P57, P58
HABD-2	G394	7.01	V55
HABD-2	S398	6.20	V52
HABD-1	N604	5.44	T43, W44
HABD-2	T397	5.31	V52
HABD-5, KGD Motif	G189	5.12	L85
HABD-3	M356	4.95	P58
HABD-4/HABD-5	H154	4.93	K74
HABD-2	Y633	4.23	V50
HABD-1	T662	4.04	W44
HABD-5	M137	3.83	L78
HABD-1	L660	3.26	W44
HABD-4	E349	2.69	E70, Y71
HABD-5	P139	2.59	L78
HABD-2	E638	1.72	N49
Linker	H108	0.92	F63
HABD-5, KGD Motif	K188	0.70	L85, H86
HABD-5	Y169	0.63	W81
HABD-5	K183	0.36	W81, T82
HABD-5	T186	0.32	L85
HABD-2	N549	0.18	W53

Supplementary Table S2. Interactions in each of the 5 EBV gH high affinity binding determinants (HABD) with gp42.

Structural feature (gH subsite)	gH residue/atom	gp42 residue/atom	Interaction type	Distance (Å)
HABD-1	F605/CD1	W44/CD1	Van der Waals	5.6
	F614/CE1	W44/CD1	Van der Waals	6.2
	I613/CD1	W44/CG	Van der Waals	3.4
	F614/CE1	W44/CZ3	Van der Waals	4.1
	I602/CD1	W44/CZ2	Van der Waals	4.7
	L660/CD2	W44/CH2	Van der Waals	4.4
	C612/O	K47/N	H-bond	2.8
HABD-2	I548/CG2	W53/CH2	Van der Waals	4.0
	I548/CG1	W53/CE2	Van der Waals	5.6
	L445/CD2	W53/CD1	Van der Waals	5.0
	P441/CB	W53/CD1	Van der Waals	3.8
	N442/OD1	W53/N	H-bond	3.0
	N442/ND2	W53/O	H-bond	2.9
	L445/CD2	V52/CG2	Van der Waals	4.8
	L401/CD2	V52/CG2	Van der Waals	4.1
	T397/CG2	V52/CG2	Van der Waals	4.5
	G394/CA	V52/CG1	Van der Waals	4.0
	E362/CB	V52/CB	Van der Waals	4.6
HABD-3	Y389/CE1	P58/CG	Van der Waals	4.0
	Y389/CG	P59/CD	Van der Waals	3.9
	G391/CA	V55/CG2	Van der Waals	4.4
	Y383/CE1	P59/CG	Van der Waals	4.8
HABD-4	Q344/CG	Y71/CE1	Van der Waals	4.3
	Y346/CE2	Y71/CZ	Van der Waals	4.4
	Q129/CG	Y71/CE2	Van der Waals	4.9
	Y346/N	Y71/OH	H-bond	3.0
	Y132/CG	Y71/CD2	Van der Waals	3.5
	Y133/OH	G72/N	H-bond	3.7
HABD-5	Y157/CD2	L78/CD1	Van der Waals	4.1
	A172/CB	L78/CD2	Van der Waals	4.0
	T170/CG2	L78/CD2	Van der Waals	4.4
	A159/CB	P79/CG	Van der Waals	3.7
	S161/OG	W81/NE1	H-bond	3.4
	Q168/NE2	W81/O	H-bond	3.7
	Q168/CB	W81/CZ3	Van der Waals	3.8

Supplementary Table S3. Cell-cell fusion assay experimental data for Figure 6.

EBV gL mutant	Surface Expression (anti-HA)			Epithelial cell fusion			B cell fusion		
	Mean	±S.D.	N	Mean	±S.D.	N	Mean	±S.D.	N
gH (neg. ctrl)	12	3	3	12	8	3	1	0	3
gH/HA-gL	100	4	3	100	4	3	100	5	3
N69D	104	13	3	106	10	3	89	6	3
N69L	99	1	3	224	40	3	113	13	3
S71V	104	6	3	272	26	3	116	15	3
N69L/S71V	95	10	3	279	70	3	93	9	3
L74A	101	8	3	71	11	3	85	15	3
L74E	97	7	3	46	11	3	97	9	3
V75N	99	7	3	71	12	3	90	11	3
I76A	98	10	3	72	10	3	94	7	3
I76D	99	5	3	70	13	3	80	8	3
R78A	91	8	3	71	9	3	84	6	3
R78L	90	10	3	52	8	3	64	9	3
R78M	101	11	3	51	6	3	88	13	3
L74A/I76A/R78A	99	5	3	42	11	3	90	11	3
Y131A	103	11	3	45	9	3	95	13	3
Y131F	100	8	3	119	5	3	79	15	3

S.D. is Standard Deviation, N is Number of biological replicates, neg. ctrl is negative control which here is gH vector alone without gL